Impact of Mars Ionosphere on Orbital Radar Sounder Operation and Data Processing

A. Safaeinili[1], W. Kofman[2], J-F Nouvel[2], A. Herique[2], and R.L. Jordan[1]

1. Jet Propulsion Laboratories, California Institute of Technology, Pasadena, CA 91109, USA.
2. Planetology Laboratory, CNRS, University of Joseph Fourier, Grenoble, France.

Abstract

Orbiting radar sounders may become the primary tools in global investigation of Mars subsurface. Orbital radar sounding of Mars is complicated by the presence of a significant ionosphere . The need to penetrate deep requires radar operation at a MHz frequency regime which make ionospheric distortions unavoidable. This paper addresses the issues that a radar sounder will face when operating close to the ionosphere's plasma frequency. Although the results of this paper are general, the main focus is Mars Advance Radar for Subsurface and Ionospheric Sounding (MARSIS) which will arrive at Mars in early 2004 aboard the European Space Agency's Mars Express Spacecraft. This paper will quantify the impact of the ionosphere on the radar sounding operation and data processing and will provide potential schemes for correcting the ionospheric distortion.

I. Background

In early 2004, the Mars Express spacecraft will arrive at Mars and will bring with it Mars Advanced Radar for Subsurface and Ionospheric Sounding (MARSIS).As its primary science objective, MARSIS will use its low frequency (HF) radar to penetrate under the surface of Mars and characterize its stratigraphy. The secondary objective of MARSIS is to characterize the ionosphere of Mars. This mission is one of three missions that will use HF radio waves to study the ionosphere, surface and subsurface of Mars. The other two missions are the Plasma Wave Sounder instrument on the Nozomi spacecraft which will arrive to Mars almost simultaneously as the Mars Express (MEX) spacecraft, and another radar sounder at higher frequency than MARSIS on board the Mars Reconnaissance Orbiter that is scheduled to arrive at Mars in 2005.

The main goal for MARSIS is to provide a global view of Mars surface and subsurface at 1-5 MHz frequency regime. MARSIS has a lateral resolution of 5 km and a depth resolution of 100 m. The operational frequency band of MARSIS spans from 100 kHz to 5.5 MHz. The subsurface sounding function can operate over four one-MHz frequency bands with center frequencies at 1.8, 3.0, 4.0, and 5.0 MHz. In each pulse repetition interval, there can be up to two pulses from either of the four frequency bands. The MARSIS instrument operates at a 130 Hz pulse repetition frequency (PRF) to allow sufficient time for a single pulse roundtrip time for spacecraft altitudes as high as 800 km. Operation at two frequency bands within a PRI will provide information about the surface and subsurface over an even larger bandwidth. The relatively wide bandwidth, which is one of the strengths of MARSIS, renders it vulnerable to the ionospheric dispersion.
The proximity of the radar sounder frequency to the ionosphere's plasma frequency makes it possible to use MARSIS as an ionospheric sounder. The ionospheric experiment on MARSIS has both active (transmit and receive) and passive (receive only) compoenent, The active ionospheric sounding (AIS) is done by using quasi-CW tones that can be swept across the entire band from 0.1-5.5 MHz. The data product of the AIS mode is an ionogram for 160 frequencies prescribed in the range of 0.1-5.5 MHz.

In the subsurface sounding mode, return echoes are recorded at a rate of 130 pulses per second and are processed on-board to form up to five synthetic apertures with two forward looking, two aft looking and one pointed in the nadir direction. The on-board processing is necessary in order to reduce the volume of the data from the spacecraft to the ground and avoid redundancy. MARSIS on-board processors perform real-time aperture synthesis while accounting for the effect of the spacecraft motion and local surface slopes.

MARSIS also provides hardware to assist in clutter cancellation. The dedicated clutter cancellation hardware includes one of the two MARSIS receive channels and a dedicated 7 meter monopole antenna in addition to its main 40 m dipole. The data from the monopole does not contain information from the nadir direction due to a null in the monopole radiation pattern in the nadir direction. As a result, an appropriately time-weighted coherent subtraction of the monopole channel from the dipole channel should reduce the amount of surface clutter in the dipole channel.

During the two-year nominal mission period, both lattitude and longitude of the MEX pericenter will change. This precession of the pericenter will result in a relatively uniform global coverage from the northern to the southern hemispheres. MARSIS operates when spacecraft is between 1200 km and 250 km (pericenter altitude) which results in only 26 minutes of operation out of nearly 7-hour orbit. At the closest approach, the spacecraft will still be at least 100 km from the region of the ionosphere with peak electron density.

In general, in the HF regime of the Radio Frequency spectrum, the depth of penetration is inversely proportional to the frequency. The minimum radio frequency is set by the ionosphere's plasma frequency. The proximity of the radar frequency to the plasma frequency will cause dispersion of the radar wave that needs to be corrected at both the instrument and ground processing steps. The plasma frequency varies with the solar zenith angle and can range from 0.5 MHz during night-time to a frequency around 3.5-4 MHz during day-time. This will limit MARSIS operation to pericenter passes with high solar zenith angles ($\theta > 90$).

II. The Impact of the Ionosphere

An electromagnetic wave propagating through the ionosphere suffers attenuation and distortion due to its complex refractive index. The attenuation is due to the electron collisions with the neutrals and ions, and the signal distortion is due to the frequency dependence of the refractive index. It is known that the plasma frequency is given by:

$$f_p = 8.98\sqrt{N_e} \qquad (1)$$

where f_p is the plasma frequency in Hz and N_e is in m^{-3}. The complex refractive index n is given by Budden, 1964:

$$n^2 = 1 - \frac{f_p^2}{f^2 - ifv} \qquad (2)$$

where f is the radio wave frequency and v is the collision frequency. The above equation can be written as:

$$n^2 = (1 - \frac{f_p^2}{f^2 + v^2}) - i\frac{f_p^2 v}{f(f^2 + v^2)}) = A^2 Exp[i\phi]$$

$$\phi = \tan^{-1}(\frac{\frac{v}{f} f_p^2}{f^2 + v^2 - f_p^2}) \approx \frac{\frac{v}{f} f_p^2}{f^2 + v^2 - f_p^2} \qquad (3)$$

where ϕ is the phase of the complex refractive index (ϕ is small). The propagation term in the medium with a refractive index of n can be written as:

$$\xi = Exp[i\frac{2\pi f}{c} nx]$$

where c is the speed of the light in free space and x is the propagation length. The attenuation factor in db/km is given by:

$$\alpha(db/km) = \frac{20000\pi \log_{10}(e)}{c}(1 - \frac{f_p^2}{f^2}\frac{2f^2 - f_p^2}{f^2 + v^2})^{0.25}\frac{v f_p^2}{f^2 + v^2 - f_p^2} \qquad (4b)$$

If we assume $f_p^2 << f^2$, then the above equation reduces to the one usually used, i.e.:

$$\alpha(db/km) = 4.61 * 10^4 N_e \frac{v}{f^2 + v^2} \qquad (5)$$

where N_e is the number of electrons per cubic centimeter. Then the total attenuation of the signal will depend on the electron density profile and collision frequency profiles. As we will see in the following section, the major difference in the attenuation calculations arises from the difference in the collision frequency.

In order to study the influence of the ionosphere on the propagating signal we need to evaluate the attenuation and distortion effects for various ionization levels, depending on the solar activity, for both diurnal and night conditions. The collision frequency depends on the neutral atmosphere profiles.

The first electron density profile used in this paper is based on Mars Global Surveyor (MGS) measurements. This profile was obtained during the day and leads to a 2.8 MHz peak plasma frequency. The second electronic density profile takes into account the hypothetical presence of meteor-origin heavy ions, leading to very large electron densities at low altitudes and therefore to very strong absorption (Witasse et al, 2001, Pesnell and Grebowski, 2000).

The other density profiles come from the Mariner 6 mission. These data correspond to a high solar activity period, so it can be viewed as a high electronic density case.
Finally, a last profile is considered: it is a night profile extracted from Mariner and Viking measurements (Mc Cormick and Whitten, 1990). The peak plasma frequency corresponding to this profile is about 600 kHz.

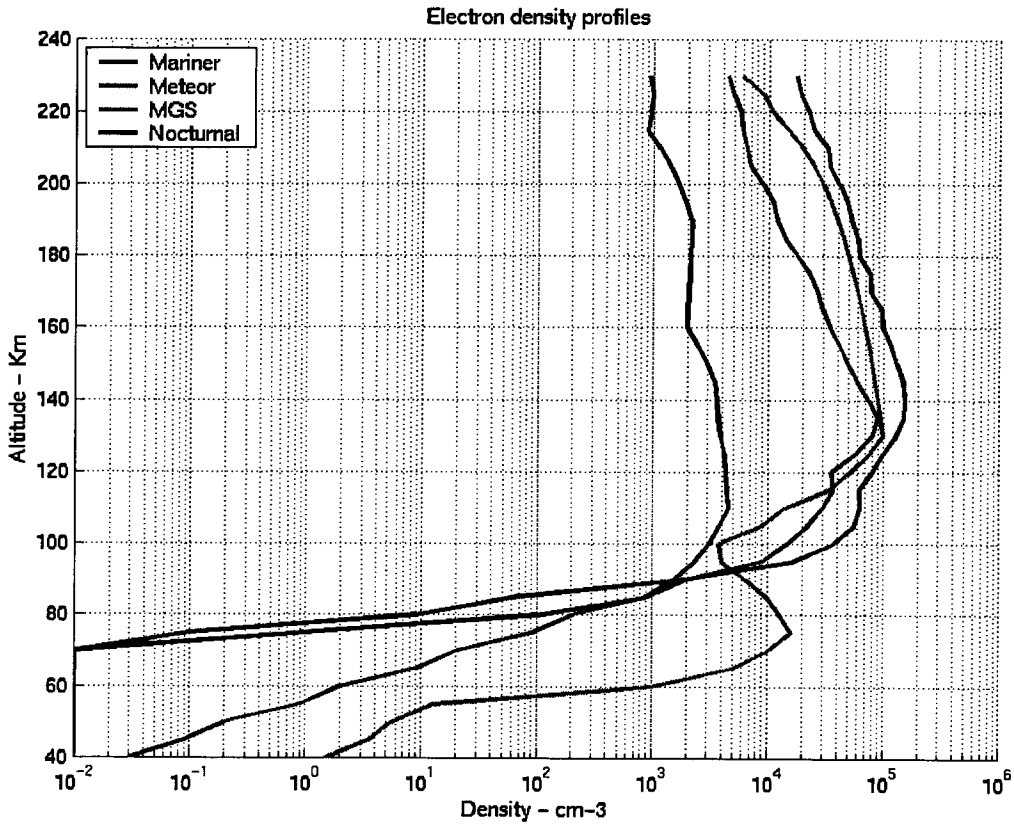

Fig. 1 : Electron density

Collision frequency

The collision frequency formula has been given by Schunk and Nagy, 1980 and Melnik and Parrot, 2000 and has different forms, thus leading to various numerical values:

Melnik :

$$\upsilon(Hz) = 2{,}12.10^{-16}.N_n(m^{-3}).T_e^{1/2} \quad (6)$$

Schunk :

$$\upsilon(Hz) = 3{,}68.10^{-14}.N_{CO2}(m^{-3}).[1 + 4{,}1.10^{-11}|4500 - T_e|^{2{,}93}] \quad (6)$$

Frequencies obtained with these two formulas are plotted in Fig. 3 (collision frequency vs. altitude).

The first expression is based on neutral density values N_n, and the second one uses the carbon dioxide density N_{CO2}. Neutral particles in the Martian ionosphere are mainly carbon dioxide ones so this difference between the two formulas is not important. Both formulas depend on the electronic temperature T_e.
These data, N_n and T_e, are extracted from three articles : [Mc Cormick & al., 1990], [Melnik & al., 1999], [Schunk & al., 1980].

Corresponding carbon dioxide density profiles are shown in Fig. 2.

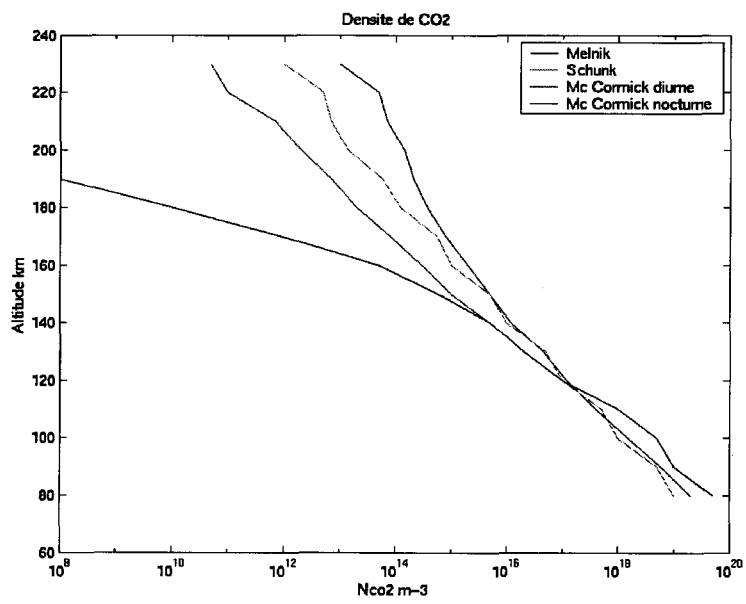

Fig. 2 : Carbon dioxide density profiles.

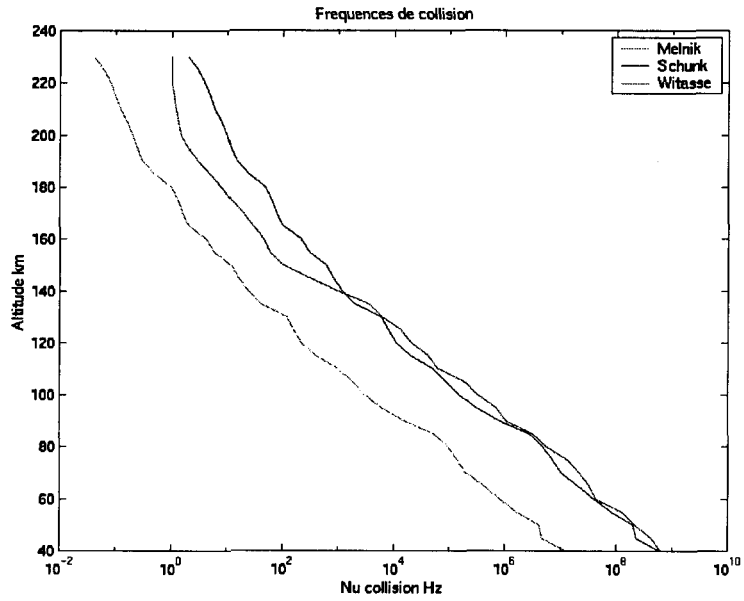

Fig. 3 : Collision frequencies

The collision frequency profiles respectively called "Melnik" and "Schunk" are plotted using respectively Melnik's and Schunk's formula. The carbon dioxide density profile used for the graph is the one we found in Melnik's article. The profile called "Witasse" uses Schunk's formula and the neutral profile is computed with values found in McCormick's paper.

We have to note here that Schunk's and "Witasse" profiles are very close at low altitudes. Moreover, Melnik's and Schunk's profiles are mainly parallel. A constant factor (about 50) separates these two profiles.

Global attenuation

We can now estimate the attenuation of the electromagnetic signal propagating through the ionosphere, using previously calculated collision frequencies and electron density profiles.

The attenuation due to the ionosphere essentially depends on the electron density profile over the bottom side ionosphere. In fact, only a small portion of the electron column density contributes to the attenuation factor of the propagating wave. Fortunately, the ionospheric attenuation is strongly frequency dependent and is observable within the bandwidth of each MARSIS band. The dependence of the attenuation on frequency is given by:

$$\alpha(f) = 4.61 * 10^4 \int_0^{Hsc} N_e(z) \frac{\nu(z)}{f^2 + \nu^2(z)} dz \quad (8)$$

where $N_e(z)$ is the altitude-dependent electron density (cm^{-3}), $\nu(z)$ is the collision frequency. In general $\nu^2(z) << f^2$, consequently, the above equation can be rewritten as:

$$\alpha(f) = \frac{4.61 * 10^4}{f^2} \int_0^{Hsc} N_e(z)\nu(z)dz \quad (9)$$

In Figure 4 we show the attenuation as a function of the frequency. As one can see, during the night, the attenuation is very low and will not limit the experiment. During the day the situation is also not very critical, except from the fact that one will have to use higher frequencies due to the plasma frequency cut off. From this figure, it is clear that if one meets the condition of the meteor profile, it will not be possible to operate MARSIS radar.
Figure 4 also points out another effect. Considering one pulse, the absorption level is a function of the wave frequency, and due to the large bandwidth signal used by MARSIS, the signal will be distorted by differential absorption. For the night condition, this distortion will be low; however it still needs to be taken into account in precise analysis.

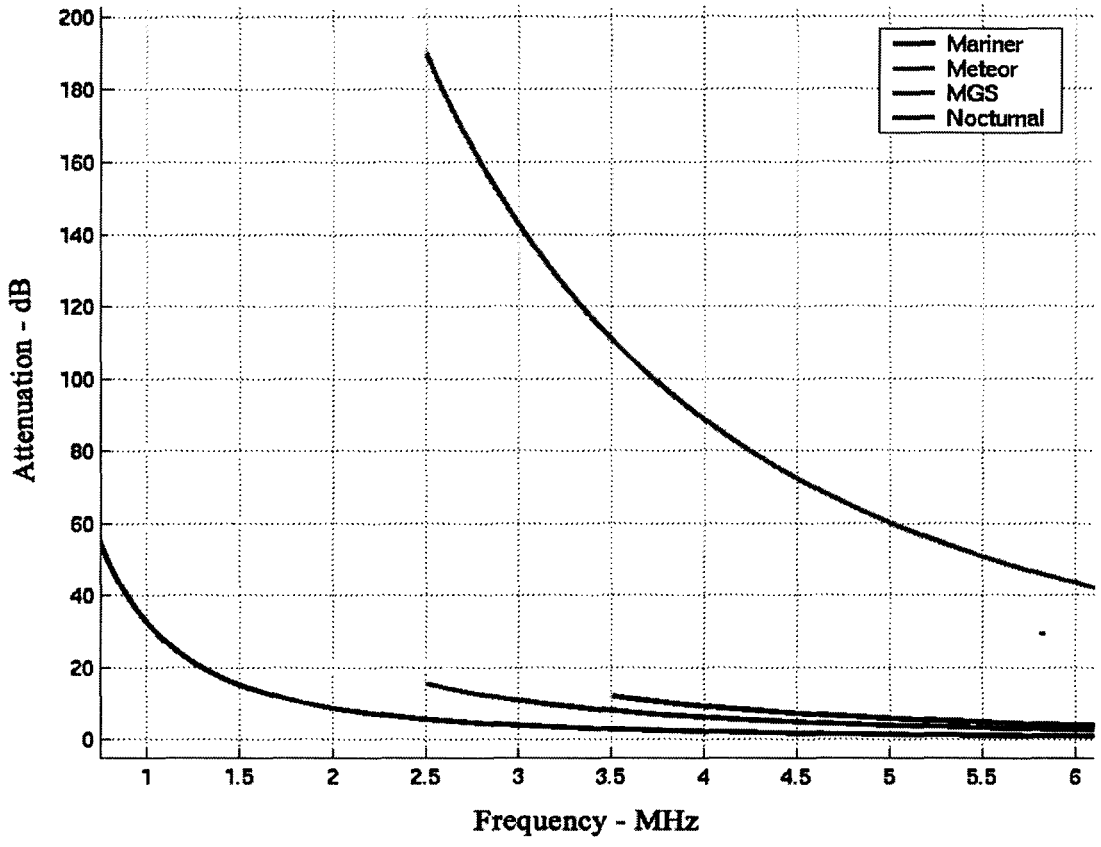

Fig. 4 : Total attenuation due to one-way ionospheric propagation
(no propagation is possible for frequencies lower than the plasma frequency)

Phase dispersion and pulse distortion

As we said before, the refractive index of the ionospheric plasma depends on the frequency. This dependence induces distortions on the propagated radio-wave: a global delay, and a pulse spreading. The echo may have its duration multiplied by a large factor (Fig. 5). The phase shift by reference to in-vacuum propagation is computed with the formula:

(10)

$$\Delta\phi(rad) = -\frac{4.\pi.f}{c_0}.\int_{z_0}^{z_1} real(n-1).dz$$

where n is the refractive index of the medium, f the signal frequencies and z0, z1 the lower and upper limit of the ionosphere where the signal propagates.
In this example we calculate the signal for the night conditions with a low frequency signal. Simulated distorted pulses after ideal chirp compression are up to 160 µs broad for a 1 µs initial signal. This signal distortion will decrease the signal to a noise ratio after signal processing and this enhances the importance of signal processing, in order to correct dispersion. In addition, the phase shift encountered along the propagation contains a non-linear term.

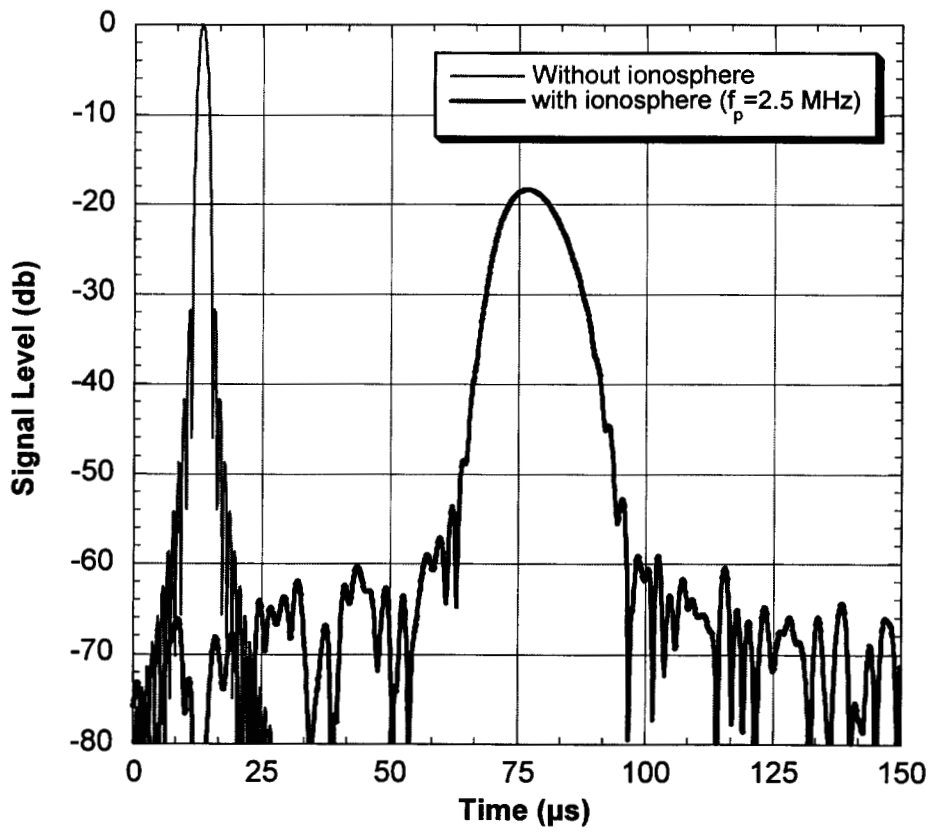

Fig. 5: Radar echo with and without ionosphere late afternoon (SZA~80 deg) profile after the ideal chirp compression. The peak plasma frequency is approximately 2.5 MHz and the radar carrier frequency is 5.0 MHz.

From these simulations, it is clear that it is necessary to find a way to compensate the ionospheric influence or to use the highest frequency band of the radar, even for night conditions.

Influence of Faraday rotation

We will provide an estimate for the expected Faraday rotation angle for linearly polarized radio waves propagating in the Martian ionosphere. These calculations take advantage of the recent vector magnetic field measurements by the Mars Global Surveyor (MGS) to provide an overall impact on MARSIS operation. The magnetic field measurements are combined with measured and/or expected ionospheric electron density profiles obtained from MGS by the radio science team to provide an estimate for strength and associated frequency of Faraday rotation angles. Considering recent magnetic field measurements, stronger than expected (as high as 1500 nT), MARSIS needs to incorporate magnetic field maps and Faraday rotation angle estimations into its operation plan. Fortunately, most of Mars (80%) has a magnetic field strength of less than 50 nT which will allow un-hindered operations over the three higher bands. Operations of the lowest band will be possible for higher solar zenith angles and areas with a weak magnetic field. Since a high electron density is a prerequisite for the Faraday rotation, the performance degradation is most likely driven by the ionospheric attenuation due to electron-ion collision than to polarization mismatch. Even for high Faraday rotation cases, the impact on MARSIS will be felt as signal fading only when the Faraday rotation angle is near 90 degrees or its odd multiples.

Faraday Rotation

The cyclotron frequency of an electron moving in a magnetic field is related to the strength of the magnetic field and is given by:

$$f_c = \frac{q_e}{m_e} B$$

where q_e is the electron charge, m_e is the electron mass and B is the magnetic field normal to the motion of the electron. The refractive index of the ionosphere without magnetic field is altered in an isotropic fashion and as a result the radio waves are slowed and attenuated. Once the magnetic field is introduced to this system, the alteration of the refractive index is no longer isotropic and will depend on the local magnetic field vector. For a circularly polarized wave, the refractive index of the medium can be expressed as:
(11)

$$n_{\pm}^{\ 2} = 1 - \frac{f_p^2}{f(f \pm f_c) - ifv}$$

Since $f_c << f$, the ionospheric attenuation equation is the same as one shown in [Safaeinili and Jordan, 2000] and does not depend on the cyclotron frequency. By decomposing the linear polarization wave into two circularly-polarized waves, the one-way polarization angle rotation rate can be written as:

(12)

$$\frac{d\Psi}{dz} = \frac{k}{2}(n_+(z) - n_-(z))$$

The above equation can be approximated by the following equation:

(13)

where B_n is the magnetic field component normal to the surface of the planet. B_n is the most

$$\frac{d\Psi}{dz} = \frac{\pi q_e}{m_e c} \frac{f_p^2(z) B_n}{f\sqrt{f^2 - f_p^2(z)}}$$

significant component for MARSIS which is a nadir-looking radar. Note that the Faraday rotation angle does not depend on the collision frequency since $v << f$. The total polarization angle rotation can be calculated by integrating the above equation over the propagation length.

(14)

$$\Psi = \frac{k}{2}\int_0^h (n_+(z) - n_-(z))dz$$

The Faraday rotation angle directly depends on the normal magnetic field and local electron density (or quadratic dependence on the plasma frequency f_p). Since the magnetic field is locally stable, the main source of variation in the Faraday rotation angle is the solar zenith angle at the time of observation. (15)

$$\Psi = 1.485*10^5 \frac{B}{f^2}\left(\int_0^h n_e(z)dz + \frac{40.32}{f^2}\int_0^h n_e^2(z)dz\right) \approx 1.485*10^5 \frac{B}{f^2} TEC$$

$$\Delta\Psi = 1.485*10^5 \frac{\Delta B}{f^2} TEC + 1.485*10^5 \frac{B}{f^2} \Delta TEC$$

As one can see from the formula 15 the Faraday effect depends on frequency. In order to be able to use the amplitude of the measured signal to determine the ionospheric parameters one should correct this effect at least for the lower band. The frequency dependent correction is given by

(16) $Amp_{corr} = \cos(2*\Psi)$

The error on this correction depends on the errors on the magnetic field and on the total electron content (15). Since the TEC will be determine with higher accuracy (a few %, see the next chapter) from the phase measurements than the magnetic field knowledge, this error will depend essentially on the error on the magnetic field because from formula 15 one can see that the relative error is given by

$\Delta\Psi/\Psi = \Delta TEC/TEC + \Delta B/B$

Figure 6 shows the cumulative probability of the normal component of the magnetic field. Which shows that for the majority of Mars, the total magnetic field is less than 50 nT. The

magnetic field with a strength as high as 1500 nT was observed for some regions of Mars. This figure indicates that the magnetic field is noticeably lower in the Northern hemisphere where 80% of the measurements were below 20 nT in comparison to 60 nT for the Southern hemisphere.

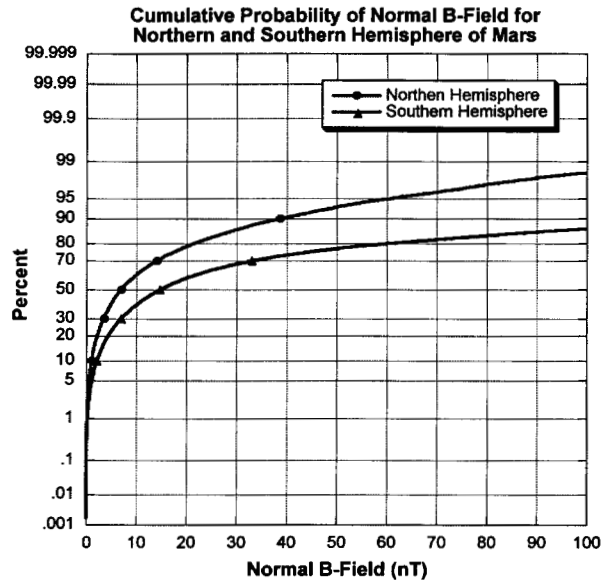

Fig. 6 : Cumulative probability distribution of the normal component of the magnetic field for the Northern and Southern hemisphere of Mars.

We calculate the Faraday rotation for the case of the low electron density peak using the profile measured by MGS (Figure 7).

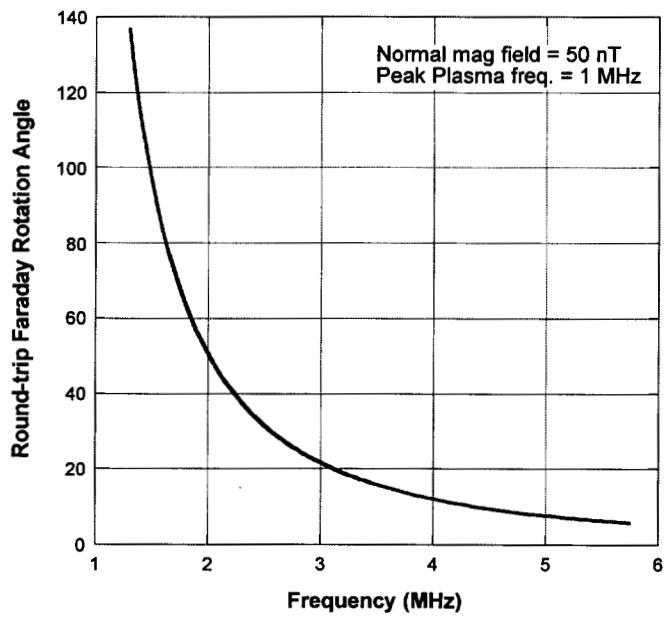

Fig. 7 : Faraday rotation for a case where the peak plasma frequency is 1 MHz with a profile similar to the one shown in Fig. 1 and a radial magnetic field intensity of 50 nT.

In the presence of a strong magnetic field, , the difference in the refractive index for two circular waves with opposite polarization causes various group delays. This will result in a differential delay in the two circular wave components. This effect is shown for a number of magnetic field strengths with a peak plasma frequency of 1 MHz. As seen in Fig. 8, this effect can be important over regions with high magnetic fields.

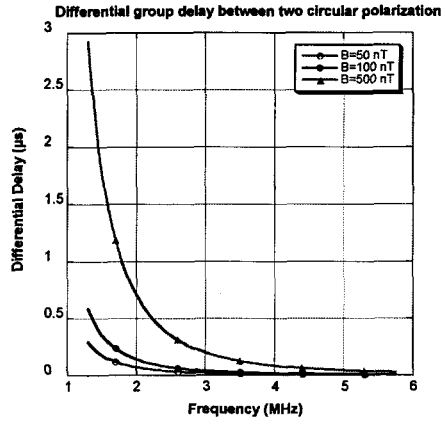

Fig. 8: Differential group delays for two circular waves with opposite polarization for three different magnetic field strengths.

The Faraday rotation is a significant factor that needs to be calculated during the operation of MARSIS. However based on our current knowledge of Martian magnetic fields and the ionosphere, the Faraday rotation is not a driving degrading factor. Under worst conditions (a large magnetic field and daytime operation), the Faraday rotation may cause fading of the MARSIS signal over the regions where the Faraday rotation is close to 90 degrees or its odd multiples.

III. Calibration Scheme

There are two categories of correction schemes that are relevant to MARSIS operation : 1) inline (real-time) calibration for on-board processing , and 2)offline calibration for optimum ground science data processing. Ideally, it is desirable to collect data in an unprocessed fashion where no corrections are applied in real-time. Real-time data corrections tend to be sub-optimal and do not provide the best science data quality. However, sometimes, it is required to perform real-time correction so that the real-time operational needs of radar such as signal acquisition and tracking are met. In MARSIS, most of the science data is not calibrated on-board but is sent to the ground for optimal ionospheric corrections. However, an on-board real-time correction scheme is needed to make radar acquisition and tracking possible. In the following, first we present a more optimal ground calibration scheme. Next, we present the Front Surface Reflection (FSR) on-board real-time adaptiveionospheric correction scheme.

Optimal Ionospheric Correction

One of the important tasks after the data acquisition is the ionospheric calibration stage which will be performed on the ground. The broadband nature of the MARSIS instrument makes it

possible to solve for the unknown ionospheric parameters. In the following, a potential scheme for this calibration process is presented.

The above equation describes the dependence of the ionospheric phase dispersion on the electron density profile. A number of observations can be made:

1. For frequencies much larger then the peak plasma frequency, the phase dispersion becomes independent of the electron density profile shape and only depends on the Total Electron Content (TEC) between the spacecraft and Mars surface
2. For frequencies close to the plasma frequency (e.g. MARSIS first band at night or all bands during daytime operation), the ionospheric phase dispersion depends on the electron density profile.

For the first case, one can simply solve for the TEC. The second case is more interesting since it provides additional information about the shape of the electron density profile. It is, however of limited value.

Ionospheric Dispersion and Attenuation Error Factor

The ionosphere of Mars affects the MARSIS signal in three distinct ways:

1. Dispersion (phase distortion)
2. Attenuation (which is also the phase dispersion because the causal signal should meet Konig-Kramer's equation)
3. Faraday rotation (effectively an attenuation due to polarization mismatch)

The effects of the ionosphere on the sounding signal will be compensated as follows:

Ionospheric Dispersion

There are two techniques which will be used to solve for this unknown. They are the Front Surface Reflection technique and the Contrast optimization technique (Picardi et al. 2001); The Front Surface Reflection technique strategy to solve for this unknown can be as follows: The first step is to match the received signal from the surface with the ideal chirp response. Then the Fourier transform of the surface reflection signal will allow the estimation of the attenuation and phase versus frequency. The measured signal spectrum is affected by a number of factors other than the ionosphere. These include 1) the system frequency response, 2) surface frequency response, and 3) the Faraday rotation. Among these, the system frequency response can be modeled to some accuracy and then measured in orbit for times when ionospheric impact is minimal and over smooth surfaces. The surface frequency response can be modeled by application of a radar equation. The Faraday rotation over a significant part of Mars is not significant, especially, for the upper frequency bands. If all three above-mentioned terms are compensated (or the compensation is negligible) , then the next step is to fit the measurements and the theoretical values of the phase and attenuation by minimizing the square distance ε (formula 23). This allows one to obtain the total electron content and the sum $\Sigma\, Ne_i * \nu_i$ over the whole ionosphere which is the column integral of the product of the electron density and the collision frequency. Since this product has significant value only in the bottom-side portion of the ionosphere, in essence, estimation of this sum will provide direction information on the electron density profile in the bottom-side portion of the ionosphere. These two parameters are obtained with very good accuracy (less than a few %).

(23)

$$f_j = \sqrt{\left(\alpha(w_j) - \sum_i \alpha_i(w_j, Ne_i)\right)^2 + \left(\varphi(w_j) - \sum_i \varphi_i(w_j, Ne_i)\right)^2}$$

$$\varepsilon = \sum_j f_j^{\,2}$$

j=1, ..., : frequency step
i=1, ...,: altitude step

$$\alpha_i = \frac{4.61*10^4}{w_j^{\,2}} Ne_i.\upsilon_i$$

$$\varphi_i = -\frac{4\pi w_j}{c_0}.real\left(\sqrt{1 - \frac{8980^2.Ne_i}{w_j^{\,2}} - i.\frac{8980^2.Ne_i.\upsilon_i}{w_j^{\,3}}} - 1\right)$$

υ_i is fixed to the collision profile

The described fitting procedure gives in principle the electron profile. However practically, the routine converges well only to the integrated quantities. To be able to obtain the electron density profile one should find very close initial conditions of the fitting. On the contrary, the estimation of the total electron content (TEC) and the sum $\Sigma\, Ne_i*\nu_i$ do not need the close initial conditions. When the Faraday effects start to be significant, it will not be possible to fit the phase and the amplitude together due to the error in the correction term resulting from the high uncertainty of the magnetic field.

The first step, in the estimation process, is to determine the TEC by fitting only the phase and neglecting the phase dependency on the $Ne_i*\nu_i$ which is of the second order. This fitting will allow the TEC determination with a few % of accuracy. Then the Farady correction (formula 15) is applied. Once this is done, the approach of the non-linear fitting for the attenuation can be seen in the following approximation. Once the two above-mentioned attenuation terms are compensated, the residual radiometric term is given by

$$A_{db}^{sig}(f) = \alpha_{db}^{ion}(f) + \Gamma_{db} \quad (25)$$

where $\alpha_{db}^{ion}(f)$ is the frequency dependent attenuation due to the electron-neutron collision frequency and Γ_{db} is the surface reflection coefficient in db.

The last step is to fit a curve of form

$$A_{db}^{sig}(f) = \frac{\eta_1}{f^2} + \eta_2$$

(26)
where

$$\eta_1 = 4.61*10^4 \int_0^{Hsc} N_e(z)v(z)dz$$

$$\eta_2 = \Gamma_{db}$$

For bands 3 and 4, where $f_0 - \Delta f < f < f_0 + \Delta f$ and $\left|\frac{\Delta f}{f}\right|^2 << 1$ then the above relationship can be written as

$$A_{db}^{sig}(\Delta f) = \frac{\eta_1}{f_0^2} + \eta_2 - 2\frac{\eta_1}{f_0^2}\frac{\Delta f}{f_0} \quad (27)$$

This equation represents a linear relationship in attenuation in db and frequency offset from the center of the band. The slope of this line is directly related to η_1 which is the column integral of the product of the electron density and the collision frequency. Since this product has significant value only in the bottom-side portion of the ionosphere, in essence, estimation of the parameter η_1 will provide direct information on the electron density profile in the bottom-side portion of the ionosphere.

The above simplified relationship can also be used to observe the sensitivity of ionospheric parameter estimation to errors in signal spectrum. The parameter η_1 is found by applying a linear fit. This means that the error is inversely proportional to the number of independent measurements (which means number of frequency) and proportional to the error on the A_{db}^{sig} which depends on SNR(f).

The accuracy in estimating the slope η_1 depends on the surface return signal spectrum SNR. Independent of any other radiometric correction, it can be shown that the accuracy is the same as the SNR after range compression. However, in reality, the error in estimating the slope parameter is dominated by systematic errors introduced by erroneous radiometric corrections such as antenna radiation efficiency, etc.

Real-Time Correction Scheme : Front-Surface Reflection (FSR) Scheme

The scheme presented in the previous section is computationally involved and can not be implemented in real-time using the limited instrument on-board processing capabilities. An effective real-time ionospheric compensation need to be adaptive and require minimum computational resources. In general, this can be a very difficult problem, but in this case, Mars presents a solution through its relatively smooth surface with a potentially strong specular reflection component. The front-surface reflection (FSR) method of ionospheric calibration is an adaptive correction scheme that exploits the smoothness characteristics of Mars surface at MARSIS operation frequencies (Safaeinili and Jordan, 2000). The principle behind this correction scheme is that a strong specular surface reflection is present as the first component of the radar echo which is a fundamental assumption on which this technique relies. This 'Front Surface Reflection' acts as the impulse response of the ionosphere which acts a dispersive filter used in the processing as a matched filter. This is a fully adaptive technique for the removal of ionospheric dispersion distortions from the radar signal.

Topography profiles obtained by MOLA (Mars Orbiter Laser Altimeter) indicates that the surface of Mars, at scales that are relevant to MARSIS experiment (>1 km horizontal scale), is very smooth and is expected to provide a very specular radar return. The FSR uses the mean surface return as the point spread function for the ionosphere and adaptively corrects for it on a frame by frame basis.

The performance of the FSR depends on a number of factors that include 1) surface smoothness, 2) Signal-to-noise ratio, and 3) the stability of the ionosphere within the imaging frame. In the following we will assume that ionosphere will remain stable within the frame, i.e. spatial stability over 5 km within a two-second timeframe.

Signal Model

The radar sounder signal is a combination of signals from four different type of sources: 1) the specular component of the surface return, i.e. the smooth surface return, 2) the surface clutter or the non-specular component of the surface signal, 3) the subsurface targets, and 4) noise which includes thermal, galactic and spacecraft generated noise (EMI). So, the radar signal can be written as

(16)

$$S(t) = \sum_{i=1}^{N_c} a^c(t_i^c) R(t - t_i^c) + \sum_{j=1}^{N_s} a^s(t_j^s) R(t - t_j^s) + R(t) + n(t)$$

Where $R(t)$ is the specular surface return (which is assumed to be the transmitted signal modified two times by ionosphere), $n(t)$ is the noise, $a^c(t_i^c)$ and $a^s(t_j^s)$ are the radar backscattering coefficient for surface clutter and subsurface respectively assuming that there is no aditional dispersion in the subsurface signal The time $t = 0$ corresponds to the time for the mean surface return. Assuming the mean specular surface return dominates the returned echo, i.e. $a^c(t_i^c) << 1$ and $a^s(t_j^s) << 1$, the compressed signal using the front-surface signal can be written as (17)

$$S^c(t) = \int (R(t') + n(t'))S(t - t')dt'$$

Or equivalently

Where $\xi(t)$ is the normalized auto-correlation of the reference signal (or compressed signal),

$$S^c(t) = \sum_{i=1}^{N_c} a^c(t_i^c)\xi(t - t_i^c) + \sum_{j=1}^{N_s} a^s(t_j^s)\xi(t - t_j^s) + \xi(t) + \frac{1}{\gamma}\zeta(t)$$

(18)

γ is the SNR and $\zeta(t)$ is the normalized auto-correlation function of the noise. The above equation shows the contributions from the surface clutter, subsurface targets, the mean surface layer and the noise (galactic and thermal).

Surface clutter and thermal noise are the two main factors in degrading the sounder performance.

Effect of the Noise

Now we explore the effect of the ideal $H(t)$ chirp compression on the correlation of the noise., which is the first step in the FSR. The compressed MARSIS radar signal can be written as

(19)

$$H(t) \otimes S(t) = H(t) \otimes \left[\sum_{i=1}^{N_c} a^c(t_i^c) R(t - t_i^c) + \sum_{j=1}^{N_s} a^s(t_j^s) R(t - t_j^s) + R(t) \right] + H(t) \otimes n(t) \quad (20)$$

Where $R(t)$ is the specular surface return, $n(t)$ is the noise, $a^c(t_i^c)$ and $a^s(t_j^s)$ are the radar backscattering coefficient for surface clutter and subsurface respectively. The time $t = 0$ corresponds to the time for the mean surface return.

$$w(t) = \int H(s) n(s - t) ds \qquad (20)$$

The last term of the above equation is the noise term for the compressed signal which we will term $w(t)$. In other words,

Consequently, the correlation function of this noise is given by

(21) $$R_w(\tau) = \iiint H(s) n(s - t) H(s') n(s - t + \tau) ds ds' dt$$

And then after reversing the order of integral and evaluation with respect to s we have

$$R_w(\tau) = \int R_n(k + \tau) R_H(k) dk$$

In other words, the auto-correlation function of noise after the first stage ideal compression is equivalent to the convolution of the auto-correlation functions of the original galactic noise and ideal reference function. Since both of these functions have very rapid drop rates for increasing shift values, the resulting correlation function will also be rapidly dropping.

The self-correlation of the noise in the extracted reference function results in no SNR gain from the chirp compression at the near surface (t close to 0), however, as time increases the SNR gain due to the range compression increases at the rate that the auto-correlation function of the noise drops. Since the thermal and the galactic noise are expected to be white noise, the noise auto-correlation function is expected to drop very rapidly. Consequently, the impact of the noise in the reference function is minimized for deep targets for which a higher SNR improvement is required.

Effect of the Clutter

In cases where the surface is rough, the clutter can mask the subsurface echoes. In general, the clutter problem is not algorithm-specific and will persist for all compression schemes equally. However, for the FSR algorithm where the reference function is extracted from the signal itself, the presence of the clutter will degrade the compression in a *benign* way. There are two types of clutter signal: 1) the continuous clutter, and 2) single clutter target.

The first case corresponds to a situation where the surface is rough and the slope rms has the probability density function $f(\theta)$. In this case, the compressed signal is degraded through a blurring operation that can be expressed in average as (22)

$$S'(t) = \int S(t-t')f(\arcsin(\sqrt{\frac{ct'}{2H}}))dt' \approx \int S(t-t')f(\sqrt{\frac{ct'}{2H}})dt'$$

where c is the speed of light, t is the time elapsed after the first mean surface return, and H is the altitude. In general, the function f() drops as time increases.

If the clutter consists of one or a finite number of strong scatterers, then the above integral will reduce to a sum of finite number of sounding profiles added together with different weight and time delay. Under this scenario, the final profile will include a number of *ghost* profiles whose strength depends on the strength of the clutter signal components.

IV. Summary

This paper presents the impact of the Mars ionosphere on the operation of MARSIS and its data interpretation. Two type of ionospheric calibration scheme was presented. The first algorithm is an optimal ionospheric calibration scheme which relies on the specularity of the surface to deconvolve the effect of the ionosphere. This algorithm is applied on the ground to calibrate the MARSIS science data in the subsurface sounding mode. The second scheme, that is called Front-Surface Reflection (FSR) technique, also relies on the specularity assumption and it is implemented in real time. As a result, it is not optimum but it can adaptively compensate for the majority of ionospheric distortion on-board in real-time.

V. Acknowledgement

The research described in this paper was carried out by the Jet Propulsion Laboratory, California Institute of Technology under a contract with the National Aeronautical and Space Administration.

VI. References

1. Budden, K.G. 'Lectures on Magnetoionic Theory', Gordon and Breach Publishing Group, 1964.
2. Witasse, O. et al, HF radio wave attenuation due to a meteoric layer in the atmosphere of Mars, Geophys. Research Letters, 28 (15), 3039-3042, 2001.
3. Pesnell, W. D., and Grebowski, J., Meteoric magnesium ions in the Martian atmosphere, J. Geophys. Res., 105, 1695, 2000.
4. Mc Cormick, P.T., and Whitten, R.C., The dynamics of the ionosphere of Mars at large solar zenith angle, J. Geophys. Res., 95, 6263, 1990.
5. Schunk, R. W., and Nagy, A. F., Ionospheres of terrestrial planets, Reviews of Geophysics and Space Physics 18, 813, 1980.
6. Melnik, O., and Parrot, M., Propagation of electromagnetic waves through the Martian ionosphere, J. Geophys. Res., 104, 12705, 1999.
7. Safaeinili, A., and Jordan, R.L., Low Frequency Radar Sounding Through Martian Ionosphere: Problems and A Proposed Solution, IGARSS 2000 held in Honolulu, Hawaii.
8. Biccari, D., et al.,, "Ionosphere Phase Dispersion Compensation", InfoCom Technical Report #002/005/01, University of Rome, Italy.